

## STUDY OF SINGLE-STRING AND MULTI-STRING AMORPHOUS SILICON SINGLE JUNCTION MODULES IN PARTIAL SHADING

Efstratios GEORGOULAS<sup>(1)</sup> Efstratios BATZELIS<sup>(1)</sup> Sotirios NANOU<sup>(1)</sup> Stavros PAPATHANASSIOU<sup>(1)</sup>

<sup>(1)</sup> NTUA, Electric Power Division, 9 Iroon Politechniou str., 15780, Athens, Greece

e-mail: st@power.ece.ntua.gr, batzelis@mail.ntua.gr

**ABSTRACT:** In this paper a complete model of a-Si:H single junction module operating in partial shading conditions is presented. It is based on the typical single-diode model, properly adjusted for reversed operation and enhanced by a term describing the recombination phenomenon. Both single and multi-string modules are studied at partial shading operation and compared on power production and shaded cells voltage level. The simulation results are experimentally validated by measurements on two modules at various shading patterns.

**Keywords:** Amorphous Silicon, Modeling, Multi-string, Partial shading, Recombination

### 1 INTRODUCTION

The amorphous silicon technology still presents relatively low efficiency, but operates more favorably at diffuse radiation and low light, as well as at high temperature and shading [1]. Already published work on hydrogenated amorphous silicon (a-Si:H) single junction module performance under partial shading is restricted to the single cell string module structure [2]-[3]. However, the multi-string structure is also a common manufacturing technique for larger modules, giving rise to the need for a detailed analysis and comparison of the two module types at partial shading conditions.

To accomplish this, a suitable model for a-Si:H single junction PV cell is used similar to [2], in which the conventional single-diode model is expanded to describe the recombination phenomenon based on [4] and enhanced by a term for reversed operation [5]. Because of their shape, the amorphous silicon cells are often partially shaded across their length, so modeling with the cell as the main building-block may be insufficient. In this paper, the partially shaded cell is treated as two subcells connected in parallel, each subcell corresponding to the shaded and unshaded part of the entire cell, simplifying the concept of [3] for one level of shade. Then, the complete model for the PV module is constituted by a system of equations describing the single and multi-string structures.

Numerous simulations have been made for various shading scenarios (horizontal, vertical and diagonal patterns), analyzing and comparing the efficiency of the two structures. Results verify that the most favorable operation is at horizontal shading and the least efficient at vertical shading, while the single-string structure is proved to be less susceptible at diagonal shading patterns compared to multi-string modules. These conclusions are verified experimentally by outdoor measurements.

The modeling approach of the PV module single and multi-string structure down to the subcell level is presented in Section 2. The partial shading analysis and comparison of the two module types at various patterns is demonstrated in Section 3. In Section 4, indicative measurements performed on two modules of the respective structures are depicted, thus validating the model, and conclusions are summarized in Section 5.

### 2 MODELING OF PV MODULE

In this section the fundamental PV cell equation utilized is presented and then the PV module system of equations is built step by step from the subcell to the entire cell, the cell string and the module.

#### 2.1 Model of a-Si:H cell

Modeling of a-Si:H technology faces certain difficulties because of the complicated phenomenon of recombination and light-induced degradation [1], [6]. It has been already shown that the typical single and double-diode model is insufficient [7], and alternative empirical models such as in [8] are not suitable for non-uniform operation. In this paper, the model proposed in [4] is utilized, which introduces a recombination term. The model is properly adjusted for reversed operation [5]:

$$I = I_{ph} - I_{ph} \underbrace{\frac{d_i^2}{\mu\tau(V_{bi} - V - IR_s)}}_{\text{recombination}} - I_s \left( e^{\frac{V + IR_s}{a}} - 1 \right) - \frac{V + IR_s}{R_{sh}} - \underbrace{b(V + IR_s) \left( 1 - \frac{V + IR_s}{V_{br}} \right)^{-n}}_{\text{reversed operation}} \quad (1)$$

where  $I_{ph}$ ,  $I_s$ ,  $a$ ,  $R_s$ ,  $R_{sh}$  are parameters of the typical single-diode model,  $d_i$ ,  $\mu\tau$ ,  $V_{bi}$  are the coefficients of the recombination term and  $b$ ,  $V_{br}$ ,  $n$  the reversed operation parameters.

The  $I$ - $V$  curve for a typical cell is depicted in Fig. 1. The form of eq. (1) supports four-quadrant modeling, being able to represent the reversed operation at negative voltage values, which is of key importance in partial shading analysis.

#### 2.2 Parameters extraction

The  $I$ - $V$  curve of two PV modules is measured, one of single-string structure and one of multi-string, at both unshaded and shaded conditions. By applying curve

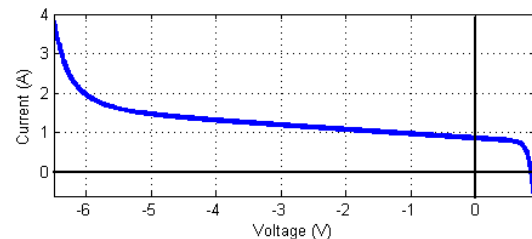


**Figure 1:**  $I$ - $V$  characteristic of a typical a-Si:H cell on all quadrants produced by eq. (1).

fitting, the parameters  $I_{ph,mod}$ ,  $I_{s,mod}$ ,  $a_{mod}$ ,  $R_{s,mod}$ ,  $R_{sh,mod}$ ,  $\mu\tau_{mod}$ ,  $b_{mod}$ ,  $V_{br,mod}$ ,  $n_{mod}$  are calculated at the module level, because of the compact fabrication of modules which does not allow single cells to be measured separately. Reduction to the cell level is accomplished by the following equations:

$$\begin{aligned} I_{ph,mod} &= N_p I_{ph,cell} & I_{s,mod} &= N_p I_{s,cell} & a_{mod} &= N_s a_{cell} \\ R_{s,mod} &= \frac{N_s}{N_p} R_{s,cell} & R_{sh,mod} &= \frac{N_s}{N_p} R_{sh,cell} \\ d_{i,mod} &= d_{i,cell} & \mu\tau_{mod} &= \frac{\mu\tau_{cell}}{N_s} & V_{bi,mod} &= N_s V_{bi,cell} \\ b_{mod} &= \frac{N_p}{N_s} b_{cell} & V_{br,mod} &= N_s V_{br,cell} & n_{mod} &= n_{cell} \end{aligned} \quad (2)$$

where  $N_s$  is the number of series connected cells and  $N_p$  the number of branches connected in parallel in the module. Typical values are assumed for the rest of the coefficients:  $V_{bi}=0.9V$  and  $d_i=0.3\mu m$  [4].

### 2.3 System of equations for the PV module

The typical single-string modules consist of cells shaped in long narrow strips, connected in series and grouped together with only one bypass diode because of the monolithic panel fabrication [3]. This fingerlike shape of cells leads to a reduced loss of performance under shade in contrast to crystalline technologies, since several cells are partially shaded, instead of a few fully shaded cells [1]. However, at highly non-uniform irradiance, the current of unshaded cells may drive the shaded ones to negative voltages, giving rise to hot strip phenomena [2], which is a limiting factor for the size of cells and therefore of modules. To structure a larger module, the

long strips have to be cut and connected in series, in more strings of smaller cell length. These cell strings are then connected in parallel, forming the multi-string module scheme (Fig.2).

Unlike the crystalline technology, the long narrow strips of amorphous silicon are usually partially shaded, which raises the need for more detailed modeling, beyond the single cell level. In [2], this problem is surpassed by assuming an average irradiance on the entire cell, but it is also admitted that this simplification is of moderate accuracy. In this paper, an approach similar to [3] is adopted, in which the PV cell is treated as two subcells connected in parallel, one for the unshaded part and one for the shaded part of the cell (Fig. 2(d)). This assumption considers one level of shade, and is based on the fingerlike shape of cells and their interconnection across their length.

Each subcell is described by eq. (1) with the appropriate parameters and operates at the common voltage of the cell  $V_{cell}$ . Therefore, the total current of the cell  $I_{cell}$  is the weighted average of the subcell currents  $I_{sh}$  and  $I_{un}$  according to the ratio of shaded to total area  $L$ . Consequently, a system of three equations is formed to model the partially shaded cell:

$$\left. \begin{aligned} f_{sh}(V_{cell}, I_{sh}) &= 0 \\ f_{un}(V_{cell}, I_{un}) &= 0 \\ I_{cell} &= L \cdot I_{sh} + (1-L) \cdot I_{un} \end{aligned} \right\} \Leftrightarrow f_{cell}(V_{cell}, I_{cell}) = 0 \quad (3)$$

The cell string consists of  $N_s$  cells connected in series operating at a common current  $I_{str}$  (Fig. 2(c)). Obviously, the total voltage of cell string  $V_{str}$  is the sum of the component cell voltages  $V_{cell,i}$ :

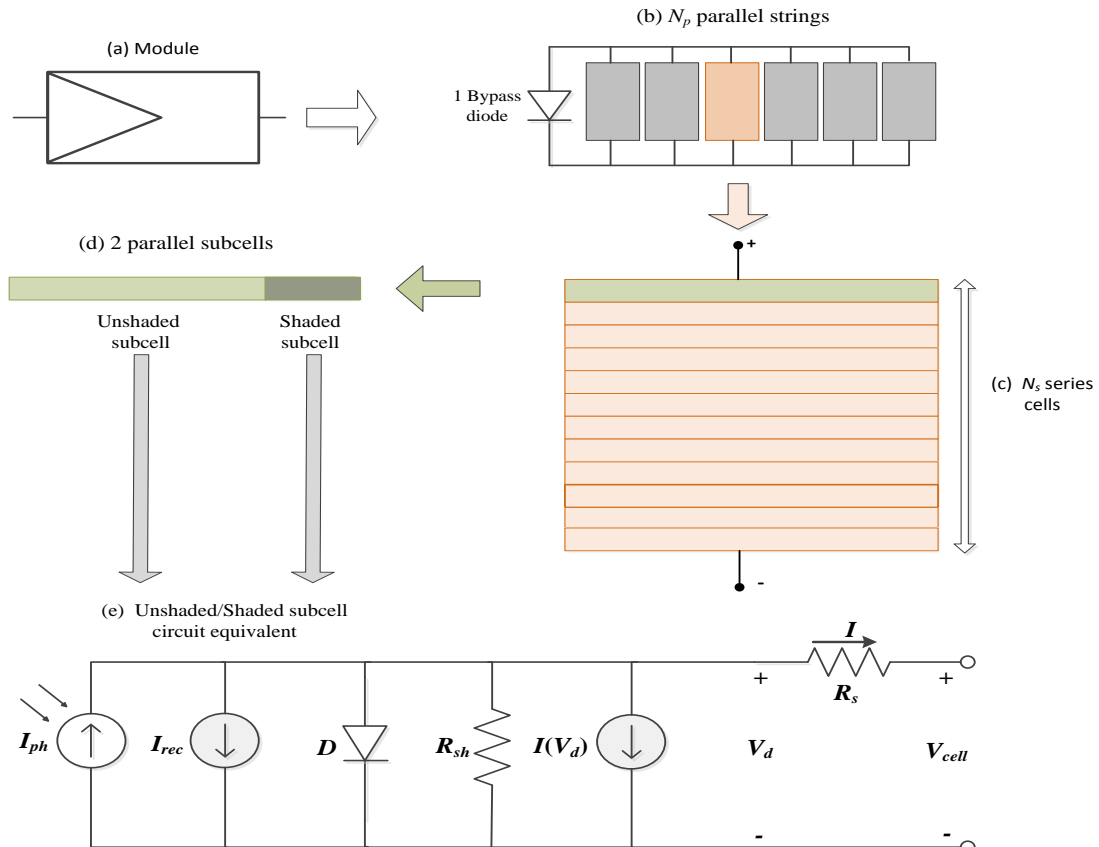


Figure 2: Multi-string module scheme.

$$\left. \begin{aligned} f_{cell\_1}(V_{cell\_1}, I_{str}) &= 0 \\ f_{cell\_2}(V_{cell\_2}, I_{str}) &= 0 \\ &\vdots \\ f_{cell\_Ns}(V_{cell\_Ns}, I_{str}) &= 0 \\ \sum_{i=1}^{Ns} V_{cell\_i} - V_{str} &= 0 \end{aligned} \right\} \Leftrightarrow f_{str}(V_{str}, I_{str}) = 0 \quad (4)$$

The single-string modules are described by the above sets of equations. However, in the general multi-string structure,  $N_p$  cell strings are connected in parallel to form a module of higher power as shown in Fig. 2(b). Then, all cell strings operate at a common voltage  $V_{mod}$  and the total module current  $I_{mod}$  is simply the sum of cell string currents  $I_{str\_i}$ :

$$\left. \begin{aligned} f_{str\_1}(V_{mod}, I_{str\_1}) &= 0 \\ f_{str\_2}(V_{mod}, I_{str\_2}) &= 0 \\ &\vdots \\ f_{str\_Np}(V_{mod}, I_{str\_Np}) &= 0 \\ \sum_{i=1}^{Np} I_{str\_i} - I_{mod} &= 0 \end{aligned} \right\} \Leftrightarrow f_{mod}(V_{mod}, I_{mod}) = 0 \quad (5)$$

The bypass diode is ignored in the above modeling approach for simplification, since it is reversely biased at the module level analysis.

### 3 PARTIAL SHADING ANALYSIS

In this Section, the partial shading phenomenon is investigated for the single and multi-string modules. Results about the power production and shaded cells stress depending on the shade pattern are extracted and a comparison between the two module types is presented. The shading ratio on all simulations is considered 40% (shaded part of module experiences 40% of the illumination on the unshaded part).

#### 3.1 Partially shaded cell

As described in the previous Section, partial shading of a cell effectively divides it into two subcells connected in parallel and operating at different irradiance levels (Fig. 2(d)). In Fig. 3, the dashed blue line is the  $I$ - $V$  curve when the cell is unshaded and the green dotted line when it is fully shaded. In all other cases, the current is the weighted average of the shaded and unshaded parts according to the shade area ratio  $L$  (eq. 3), presenting  $I$ - $V$  curves in between the unshaded and fully shaded ones. This means that partial shading in a cell affects it in a proportional manner to the shaded area, thus validating the simplified approach of modeling it as a uniformly illuminated cell operating at average irradiance.

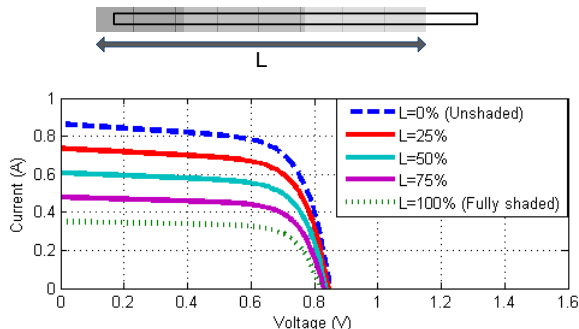


**Figure 3:**  $I$ - $V$  characteristics of a partially shaded cell for various shaded areas.

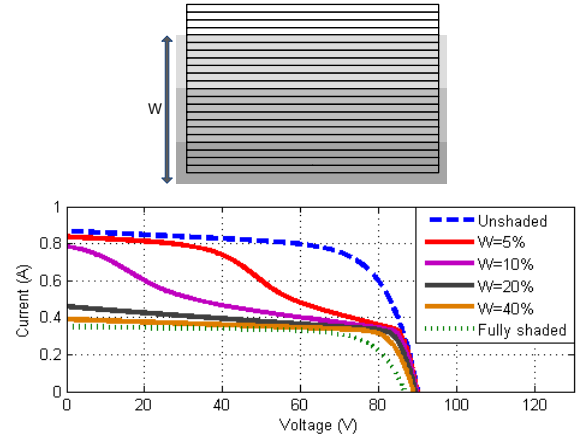


**Figure 4:**  $I$ - $V$  characteristics of a partially shaded cell string for various shaded areas.

#### 3.2 Partially shaded cell string

Since all cells in a cell string carry the same current, at partial shading conditions the unshaded cells operate at reduced current, restricted by the current of the shaded cells. In Fig. 4, a cell string of 106 cells of the single-string study case module is simulated for an increasing number of shaded cells (cells are either fully shaded or unshaded). Unlike the cell, partial shading in a cell string affects it in a strongly non-linear way, significantly reducing the current produced even for a minimum number of shaded cells. It is worth mentioning that the untypical curvature of the red and purple lines is due to shaded cell operation in the breakdown area, giving rise to hot strip phenomena.

#### 3.3 Partially shaded single and multi-string modules

In Fig. 5, study case PV modules, both multi-string (continuous lines) and single-string (dashed lines), are simulated at partially shaded conditions, considering various shade patterns.

For the horizontal shading patterns of Fig. 5(a) the modules present identical response. In the single cell string, all cells are illuminated in the same way and they may be treated as a single oversized partially shaded cell following the trends of Fig. 3. Similarly, the multi-string module consists of unshaded and fully shaded cell strings connected in parallel, that correspond to the unshaded and shaded part of an extra large partially shaded cell.

The two modules respond similarly for the vertical shading patterns, as well (Fig. 5(b)). The single-string module contains unshaded and fully shaded cells connected in series, operating as discussed in Section 3.2. In a multi-string module, all cell strings are illuminated in the same manner, each one having unshaded and fully shaded cells, thus operating as a single string of larger cells.

However, for the diagonal patterns of Figs. 5(c)-(e), the single-string module performs slightly better, as the partial shading of large cells reduces somewhat the effect of the shade, compared to the smaller but fully shaded cells of the multi-string module. This is attributed to the non-linear dependence of the cell string response on the shaded area. In the multi-string case, some cell strings are unshaded but the rest of them have fully shaded cells, significantly reducing their output as already shown in Fig. 4. On the contrary, the single cell string consists of partially shaded cells, each one operating as uniformly illuminated at the average irradiance, thus reducing the

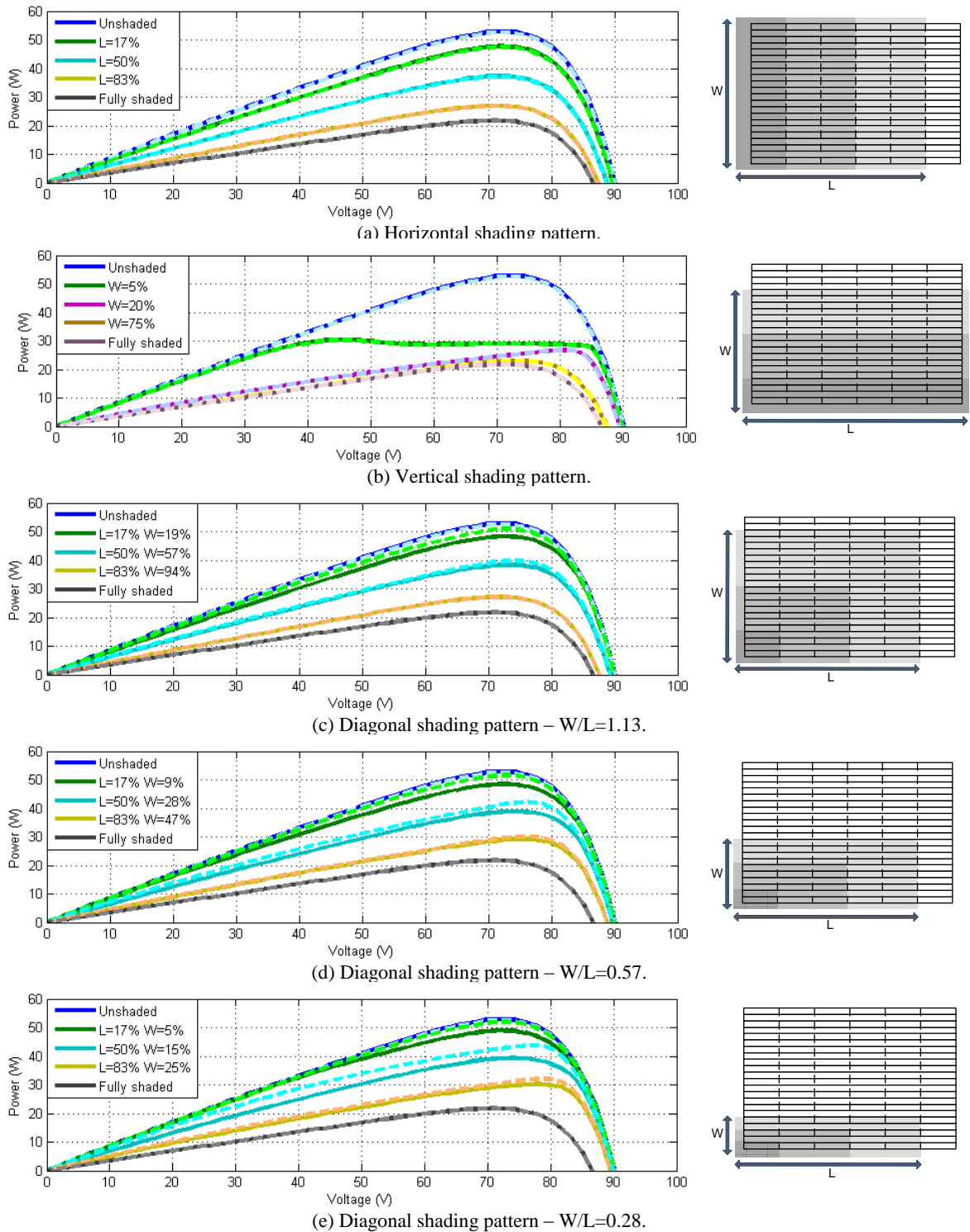


**Figure 5:** *P-V* characteristics of partially shaded modules for various shading patterns. Continuous lines correspond to multi-string module, dotted lines to single-string module.

diversification of the unshaded and shaded components. Therefore, the loss caused by the common current restriction is mitigated and shaded cells are not driven to negative voltage operation.

In Fig. 6(a), the maximum power output of the two modules is plotted for the above shading pattern over the shaded area. As expected, the power output is linearly affected by the shaded area at horizontal shading (blue lines), since the whole module behaves like a single

partially shaded cell, as already discussed. This is the most favorable shading scenario. On the contrary, when vertical shading is considered (green lines), the module power reduces very fast as the area of shade extends, due to the series connection of shaded and unshaded cells, presenting a drastic decrease for an affected area as low as 10% of the module surface.

Diagonal patterns lead to an intermediate response, with the single-string module operating slightly more

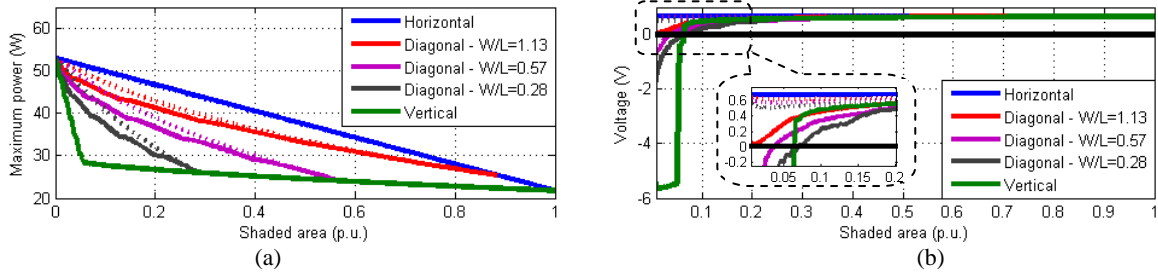


**Figure 6:** (a) Maximum power output and (b) shaded cells operating voltage in a partially shaded module vs. the shaded area for various shading patterns. Continuous lines correspond to a multi-string module, dotted lines to a single-string module.

efficiently. For large values of width to length ratio  $W/L$ , the diagonal shading pattern approaches the horizontal one, while for small values of the ratio it resembles the vertical shading scenario. This is illustrated in Fig. 6(a), in which the curves of the diagonal patterns converge to the boundary lines of horizontal and vertical scenarios, until they totally coincide.

In Fig. 6(b), the shaded cell operating voltage is plotted versus the shaded area, for the shading patterns studied. In horizontal patterns (blue lines) the shaded cells are not stressed at all, since they are all illuminated the same way in each cell string. The latter happens at the vertical shading scenario (green lines). The unshaded cells drive the fully shaded cells to negative voltages due to the common current restriction at small values of the shaded area.

In the above cases, the shaded cells of the two module types are similarly stressed. However, at the diagonal shading patterns the shaded cells of the multi-string module operate at significantly lower voltage than the single-string, which turns to be negative for small values of the shaded area. It is worth noting that, as the diagonal pattern approaches the vertical scenario, the stress of the multi-string module converges to the boundary green line, while the single-string module seems to be much more resistant, its cells always operating at positive voltage.

Comparing the two module structures, when the shade extends in a horizontal or vertical manner they present practically identical characteristics. On the other hand, in case of diagonal shading scenarios the single-string module is more efficient. This is due to the longitudinal shape of the cells, which leads to several partially shaded cells, rather than a few fully shaded ones. The shaded and unshaded components of a partially shaded cell are connected in parallel, so the response approaches that of a uniformly illuminated cell at an intermediate irradiance, according to the shaded area and irradiance ratios (this is true in most cases). In this way the impact of shading is mitigated.

#### 4 EXPERIMENTAL VALIDATION

Series of measurements were performed to validate the model used in this paper. Two modules were measured, a multi-string and a single string one, at several shading scenarios in clear sky conditions. Two semi-transparent materials with transparencies of 40% and 26% were used to emulate the shading patterns, and a variable resistor and LabView© based DAQ equipment were utilized to record the  $I$ - $V$  curves.

In Fig. 7, the measured (dots) and simulated (continuous line)  $I$ - $V$  curves of the study case multi-string

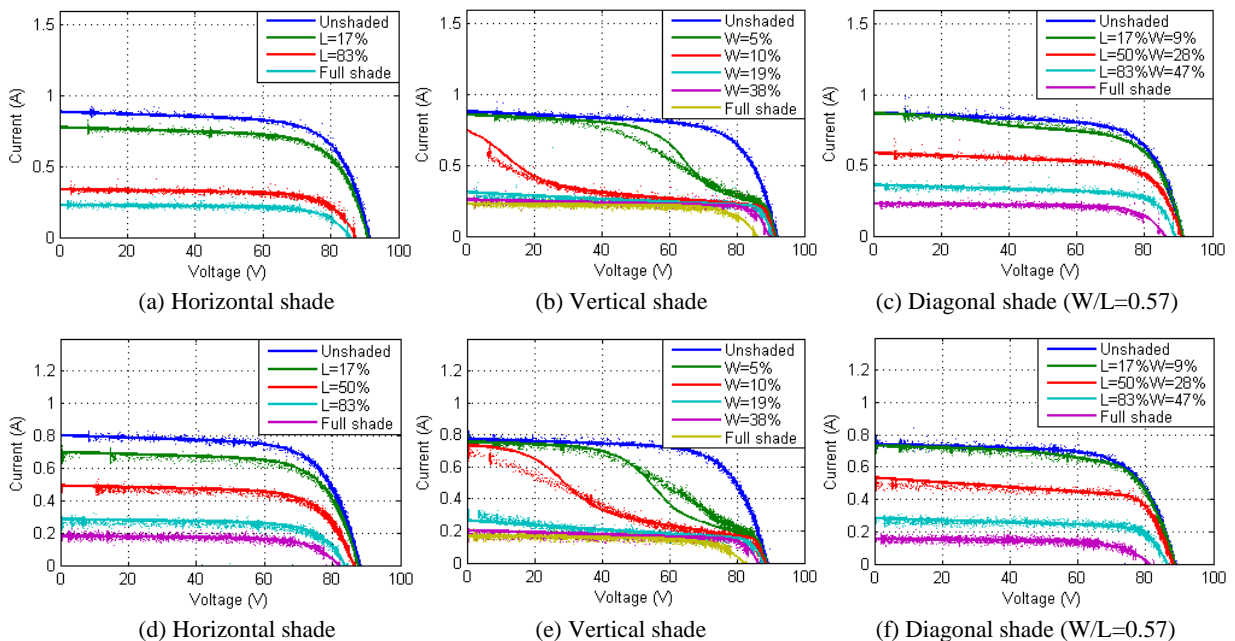


**Figure 7:** Measured (dots) and simulated (continuous line)  $I$ - $V$  curves of (a)-(c) multi-string and (d)-(f) single-string a-Si:H modules at horizontal, vertical and diagonal shading patterns (shade ratio 26%).

and single-string modules are shown for indicative shading scenarios. The agreement between measurement and simulation is satisfactory, confirming the validity of the model and analysis performed. Small deviations are present for certain vertical patterns, when too few cells are shaded. This is due to the practical difficulty to accurately emulate the shading scenario when 5 or 10 (out of 106) very thin cells need to be covered by the shading material, as well as to the inherent difficulty in determining precisely the reverse operation parameters via curve fitting on measurements, when the breakdown operation area is hardly discernible in most of the measured  $I$ - $V$  curves.

## 5 CONCLUSION

In this paper, a complete model for a-Si:H single junction modules is presented, suitable for simulating operation at partial shading conditions. The granularity of the modeling extends below the level of the single cell and the basic modeling equation describes the recombination phenomenon and reversed operation.

The model is used to study both single and multi-string modules at partial shading conditions. Results show that partial shading of a-Si:H single junction PV modules causes a reduction in output power strongly dependent on the shade pattern, as well as on the area and intensity of the shade. Vertical shading patterns have a more drastic effect, while horizontal patterns are characterized by a linear decrease of the maximum power with the shaded area. The single and multi-string module structures perform similarly, with the first one exhibiting slightly better efficiency in diagonal shading scenarios.

## 6 REFERENCES

- [1] The German Energy Society, "Planning and installing photovoltaic systems: a guide for installers, architects, and engineers", 2<sup>nd</sup> ed., Earthscan, London, 2008, pp. 41-42.
- [2] . Johansson, R. Gottschalg, and D.G. Infield, "Modelling shading on amorphous silicon single and double junction modules", 3<sup>rd</sup> World Conference on Photovoltaic Energy Conversion, Osaka, Japan, May 2003, vol. B, pp. 1934-1937.
- [3] S. Dongaonkar, and M. A. Alam, "A Shade Tolerant Panel Design for Thin Film Photovoltaics", Birck and NCN Publications, paper 859, 2012.
- [4] J. Merten, J. M. Asensi, C. Voz, V. Shah, R. Platz, and J. Andreu, "Improved Equivalent Circuit and Analytical Model for Amorphous Silicon Solar Cells and Modules", *IEEE Transactions on Electron Devices*, vol. 45, pp. 423-429, 1998.
- [5] J. W. Bishop, "Computer simulation of the effects of electrical mismatches in photovoltaic cell interconnection circuits", *Solar Cells*, vol. 25, pp. 73-89, 1988.
- [6] E. Sanchez, J. Izard, and M. Dominguez, "Experimental Study of Light-Induced Degradation in a-Si:H Thin-Film Modules under Different Climatic Conditions", 27<sup>th</sup> European PV Solar Energy Conference and Exhibition, Frankfurt, Germany, Sep. 2012, pp. 2503-2506.
- [7] M. Prorok, B. Werner, and T. Zdanowicz, "Applicability of equivalent diode models to modeling various thin-film photovoltaic modules in a wide range of temperature and irradiance conditions", *Electron Technology*, vol. 37-38, pp. 1-4, 2006.
- [8] M. Nawaz, "Computer modeling of micromorph aSi/aSiC/cSi based solar cells", 27<sup>th</sup> European PV Solar Energy Conference and Exhibition, Frankfurt, Germany, Sep. 2012, pp. 2696-2700.